

Influence of substituents in vinyl groups on reactivity of parylene during polymerization process

Sylwia Freza¹, Piotr Skurski¹, and Maciej Bobrowski^{2,*}

¹ *Department of Chemistry, University of Gdańsk, Sobieskiego 18, 80-952 Gdańsk, Poland*

² *Department of Technical Physics and Applied Mathematics, Gdańsk University of Technology, Narutowicza 11/12, 80-233 Gdańsk, Poland*

Abstract

The MCSCF calculations indicate that both triplet and singlet state of biradical di-para-xylylene can exist during polymerization of parylene in gas phase and both can potentially react with vinyl molecules. The singlet-state open-shell dimer turned out to exhibit multiconfigurational character. In the case of triplet state of the dimer two mechanisms of the reactions with various species containing vinyl groups have been examined at the B3LYP/6-31G level. The kinetic and thermodynamical barriers have been estimated for the reaction path involving the π -bond cleavage as well as for the route describing the hydrogen atom transfer. It was found that the overall reactions are thermodynamically favorable whereas appropriate kinetic barriers for certain derivatives are very small (close to 0 kcal/mol) which in turn makes allowances for easy reactivity under accessible conditions. The calculated mechanisms indicate the influence of substituents in vinyl groups for reactivity of parylene during LPCVD process.

* corresponding author, email address: mate@mifgate.mif.pg.gda.pl

1. Introduction

Poly-para-xylylene based polymers, also known as parylenes, are polymers that can be deposited in thin film form at room temperature by chemical vapor deposition (CVD). Parylene was synthesized for the very first time by Szwarc in 1947 using rapid flow pyrolysis of p-xylene under reduced pressure¹, however, the yield of this process was very low (not exceeding few percent) even at very high pyrolysis temperature. A much more effective method was proposed by Gorham in 1966² who used cyclo-di-p-xylylene ([2,2]paracyclophane) as a substrate. According to Gorham, 100% of cyclo-di-p-xylylenes are cracked into monomers which next take part in polymerization one unit at a time (this process has been termed LPCVD, Low Pressure CVD)³ at temperature above 550°C and at pressure less than 1 Torr. In 1958 Errede and Szwarc⁴ published qualitative description of the polymerization process which starts from the reaction of two monomers leading to a biradical dimer which in turn can react with another monomer unit leading to biradical trimer, and so on. In each step a biradical dimer or longer chains are needed to react with another unit. The process requires neither solvents nor catalysts and thus allows to produce non-polluted thin films of polymer over a wide range of materials, including liquids with uniform replication of the shape of its droplets⁵. Moreover, the polymerization itself occurs at room temperature which thus effectively spreads the opportunity of applications in electronics, optics and medicine⁶⁻⁹. Recently, parylene polymers are widely used for the coating of circuit boards, hybrid circuits, in production of semiconductors, capacitors, miniature electrical components, for barrier coatings, in corrosion control and as dry lubricants^{10,11}.

To improve useful chemical functionality of parylenes a lot of processes have been developed but main ideas can be grouped into two threads. One is modification of [2,2]paracyclophanes before polymerization and after following vapor deposition one can obtain functionalized chains of parylene^{12,13}. The second method is to use suitable substrate with molecules capable of reacting with non-modified monomers or biradicals during the CVD polymerization leading to modified layer of parylene over the reactive substrate. The former method requires changing of process parameters and most likely influences the morphology of the polymer film^{14,15} while the latter technique does not.

Most recently, it was experimentally proven that during the LPCVD of parylene over unsaturated fluorenes¹⁶ one can observe chemical functionalization of parylene films. The



authors concluded that the functionalization is based on chemical reaction of double bonds with xylylene radicals during deposition process. They reported the first results of chemical surface modification of poly(2-chloroxylylene), also known as Parylene C, through reactions with organic and polymeric compounds bearing double bond(s) in combination with fluorene fragments, which are responsible for novel photophysical properties of materials obtained. In our work we go a step further and try to explain the mechanisms of reactions of parylene with vinyl groups during the LPCVD. In addition, we discuss the factors influencing the reactivity of potential substrate during the deposition. For a better understanding of the reactivity we also used substrates which are gases under the deposition conditions and normally should not be considered as reactants. However, such simple models allow for the explanation of mechanisms of the vinyl groups reactivity during deposition of parylene.

Vinyl copolymerization reactions in gas phase have been extensively studied, both experimentally and theoretically. In those studies main focus was on the derivation of rate coefficients of the reactions. In particular, the rate constants of radical polymerization reactions were put in order to detail¹⁷. Generally, there were various schemes of representation of rate constants of radical¹⁸⁻²² as well as ionic polymerization²³. There were also attempts to avoid the problem of assignment of numerical parameters for particular vinyl monomers to accurately define rate constant. Instead of this, general trends of reactivity as a function of properties of substituents were observed. Evans et al.²⁴ observed a regularity that the weaker the bond to be broken the lower the activation energy barrier of the reaction. In their report, two main causes of changes in potential energy profiles of reactions involving double bonds and radicals were indicated: (a) the influence of substituents on the electron distribution and hence the charge distribution of the reacting centers, and (b) the influence of the repulsion forces between centers not directly involved in the reaction (steric terms). They also noticed the influence of substituents entering into conjugation with electrons of double bonds. Recently, similar effects were also observed by Filley et al.¹⁸ in their studies on ethylene - vinyl acetate radical copolymerization, supported by quantum chemical calculations.

The novel method of chemical functionalization of parylene films, i.e., the chemical reactions of parylene during LPCVD with substrates (liquid and solid), is indissolubly tied up with heats of vaporization (ΔH_{vap}) and heats of sublimation (ΔH_{sub}). The values of ΔH_{vap} in the literature²⁵ for common substances reveal that for larger molecules and in the case of stronger intermolecular interactions the ΔH_{vap} increases from approximately 2 kcal/mol for methane to ca. 5 kcal/mol for butane and from approximately 8 kcal/mol for methanol to ca.



10 kcal/mol for water. These values indicate that when a sufficiently low kinetic energy barrier characterizes the reaction profile the enthalpy of vaporization or sublimation can be the most appreciable.

2. Methods

2.1. Model compounds

In our calculations we used diversely substituted vinyl molecules $\text{CH}_2=\text{CHX}$ as species reacting with para-xylylene dimer (DPX). The substituents X have been chosen arbitrarily and in our work the X stands for H, Cl, Br, CN, CF_3 , NO_2 , C_6H_5 , C_6F_5 , $\text{Si}(\text{CH}_3)_2\text{-NH-SiHCH}_3\text{-NH-CH}_3$, $\text{SiNH}_2\text{CH}_3\text{-NH-SiHCH}_3\text{-NH-CH}_3$, COOC_6F_5 , COOCHCl_2 , and $\text{COOC}_4\text{H}_8\text{OH}$. The chosen set of reactants includes ethylene substituted with halogen atoms and groups possessing a set of conjugated double bonds (acrylates, phenyl and phenyl derivatives and nitro groups) in order to demonstrate the influence of substituent's electronegativity as well as conjugation with double-bond electrons on the overall reactivity. Also larger groups located in the proximity to the reacting centers were amidst the substituents to demonstrate the influence of steric effects on the reactivity of vinyl groups.

2.2. Quantum-chemical computations

The calculations were carried out at various levels of theory. MCSCF methods were used to compare energies of singlet and triplet state of biradical di-p-xylylene. In particular, CASSCF(2,2) with two SOMO orbitals and two electrons as well as MCSCF(14,14) with additional six π orbitals together with six electrons and six π^* orbitals of two aromatic rings were used. In the case of MCSCF(14,14) we took into account single and double excitations within CAS. Also, in order to improve effectiveness, the C_2 -symmetry of DPX was imposed while performing all MCSCF calculations, however, the analogous calculations were repeated later without any symmetry constraints. The geometries of singlet and triplet state of DPX were fully optimized in the latter scheme. All the MCSCF calculations were performed with the use of 6-31G(d) Pople-style basis set^{26,27}.

Density Functional Theory (DFT) with Becke's Three Parameter Hybrid Method with the LYP (Lee-Yang-Parr) correlation functional (B3LYP)^{28,29} as well as Hartree-Fock (HF)



methods were used to obtain the potential energy profiles of reactions of biradical di-p-xylylene with vinyl moieties. The corresponding transition states were located by calculating the energy profiles of the reacting systems in internal coordinates most closely approximating the appropriate reaction coordinate, with optimization of all remaining degrees of freedom. The geometry corresponding to the maximum in the energy curve was taken as an initial approximation to that of the transition state and then the gradient norm was minimized to complete the search of this transition state. The Hessian matrix and subsequently the normal modes were calculated for all stationary points. The DFT and HF calculations were performed with the use of 6-31G Pople-style basis set^{26,27}.

Transition state theory was used to utilize the entropies (ΔS^\ddagger) and enthalpies (ΔH^\ddagger) of activation to obtain Arrhenius factors and rate constants (k_{298}) for the reactions, as shown in the equation (1)³⁰, where k is the Boltzmann constant, T is the temperature (298.15 K), and h stands for Planck's constant. For all reactions, the electronic energies obtained from B3LYP and UHF calculations were corrected by the thermal and zero-point energy corrections to obtain the enthalpies of reactions leading to transition states.

$$k_{298} = kT / h \exp(\Delta S^\ddagger / R) \exp(-\Delta H^\ddagger / RT) \quad (1)$$

All calculations were performed with the Gaussian03³¹ and GAMESS³² packages.

3. Results

3.1. Open-shell singlet vs. triplet state of DPX

MCSCF/6-31G(d) energy differences between triplet and singlet state of di-p-xylylene with and without C_2 -symmetry imposed are assembled in Table 1, while the dominant configuration state functions (CSFs) of all MCSCF-generated states are assembled in Table 2. The C_2 -rotation-axis was chosen to pass through the center of the middle aliphatic C-C bond of DPX (perpendicular to this bond). The symmetry constraints enabled to perform the MCSCF(14,14) calculations where the number of symmetry adapted configurations was very large (more than 10 000 configurations). However, one should keep in mind that the DPX does not possess any symmetry during polymerization process. The geometrical structure of the biradical DPX obtained with the B3LYP method was found to be significantly twisted,

i.e., the two xylylene monomers are located almost perpendicular to each other. However, the energy barrier for rotation around the central aliphatic C-C bond is not expected to be very large (i.e., should be easy to overcome during thermal movements)³³ while even simple symmetry imposition significantly reduced computer resources needed for expensive MCSCF calculations.

An analysis of the results gathered in Table 1 revealed that the geometry optimization performed with symmetry constraints leads to very significant differences between triplet and singlet state, favoring triplet state over singlet state dimer during polymerization process. Analogous results for geometry optimization without any symmetry constraints show that the energies of triplet and singlet states are very similar and after calculations with larger active space (MCSCF(14,14) with single and double excitations) the difference of these two energies does not exceed 2 kcal/mol. Analogous results were obtained by Smalara et al.³⁴ who found at semiempirical level that the triplet and singlet states of di-p-xylylene have similar energies.

The singlet open-shell dimer of DPX is multiconfigurational. Analysis of dominant configuration state functions in the basis of natural orbitals (see Table 2) reveals that in the case of singlet open-shell state and without any symmetry constraints there are two configurations with coefficients greater than 0.6 in absolute value in the case of MCSCF(14,14) with single and double excitations, and greater than 0.7 in the case of CASSCF(2,2). Moreover, these two configurations correspond to two ionic states where the negative charge is once at one end of the dimer and next at another one, but none of these states exists solely in gas phase (which was also found by Smalara et al.³⁴). However, there were also publications indicating that ionic version of the parylene polymerization³⁵ is possible, but only when undertaken under special conditions in polar solvents.

The configuration with doubly occupied π orbitals and one electron on each SOMO does not even possess coefficients larger than 0.1. In the case of triplet-state dimer only one (biradical) configuration dominates. However, when the C_2 -symmetry was imposed (see Table 2), the ionic configurations does not appear like it was in the case of MCSCF without symmetry constraints and most likely this is the main reason of so high energy difference between the singlet states when optimized with and without symmetry constraints. The occupation numbers of two SOMO orbitals (see Figure 1) in the case of triplet state are exactly one, and in the case of singlet state are close to one. Occupation numbers of π and π^* orbitals of two aromatic rings of DPX are close to 2 and 0, respectively, in the case of triplet as well as in the singlet state.



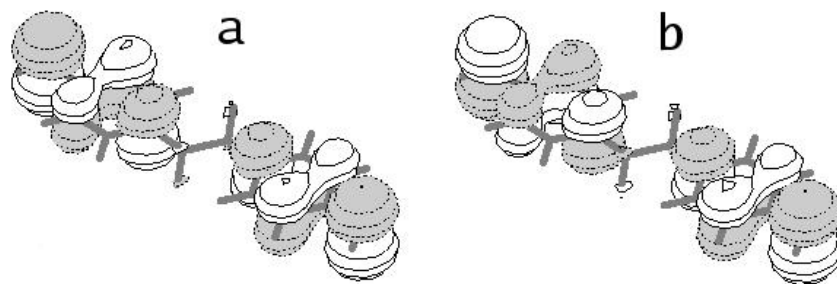


Figure 1. Singly-occupied biradical orbitals (symmetrical (**a**) and antisymmetrical (**b**)) of di-*p*-xylylene obtained at the MCSCF(14,14) level with single and double excitations with the natural orbitals basis. The occupation numbers are as follows: singlet-state dimer optimized without symmetry constraints - orbital **a**: 1.03; orbital **b**: 0.97, optimized with the C_2 -symmetry imposed – orbital **a**: 1.24; orbital **b** 1.23; in the case of triplet-state dimer both orbitals are singly-occupied.

The MCSCF calculations show that both triplet and singlet states of the dimer can exist during polymerization of parylene in gas phase and both states can potentially react with double-bond molecules. However singlet-state biradical dimer, due to its multiconfigurational nature, requires very time-consuming calculations. Moreover, the π and π^* orbitals of two aromatic rings should be taken into account. Additionally, in the case of reaction-profiles searching with DPX involved one can assume that π and π^* orbitals of two aromatic rings would play an important role and one should take them into account while constructing CAS. But in this case also additional orbitals and electrons of the second substrate should be included in the CAS which makes this type of calculations undoable (regarding the computer resources available at hand).

Therefore, we considered the triplet state of the *p*-xylylene dimer while investigating the reactions with vinyl moieties.

3.2. The reactions of biradical DPX with vinyl molecules

The *ab initio* calculations performed to explore the mechanisms of the reactions of biradical di-*p*-xylylene in its ground triplet state with various molecules possessing double bonds (C=C) were undertaken at the B3LYP/6-31G level while the HF/6-31G calculations were performed for comparison.

In the case of gas-phase reactions involving similarly substituted species and utilizing the same mechanism the major factor which influences the reactivity is the kinetic activation barrier. At room temperature the polymerization reactions are

characterized by sufficiently low kinetic activation barriers^{3,4,34}. Hence, the search for the appropriate and most feasible mechanism for the reaction of molecules containing the C=C double-bond with parylene requires the investigation of energy profiles for each reaction (in particular the relative energies in transition states at reaction paths). We considered two possible mechanisms for the $\cdot\text{DPX}\cdot$ reacting with unsaturated $\text{CH}_2=\text{CHX}$ molecules. One of them (the straightforward attack on the vinyl carbon atom) is expected to lead to the consecutive copolymerization since a biradical species is generated as its product while the other one (the hydrogen atom attachment/detachment) should lead to the final product without further reactions.

3.2.1. Straightforward electrophilic attack on the vinyl carbon atom

The first mechanism considered for the $\cdot\text{DPX}\cdot$ reacting with a compound containing C=C double-bond is the straightforward electrophilic attack on the vinyl carbon atom (see routes A and A' in Figure 2).

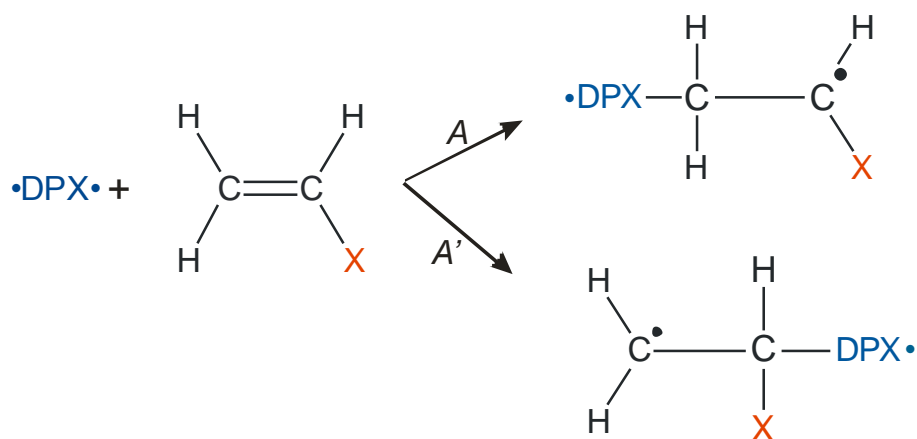


Figure 2. The mechanism A / A' involving the π -bond cleavage

According to this mechanism, the π -bond in the $\text{CH}_2=\text{CHX}$ breaks which is followed by the attachment of the molecule to the $\cdot\text{DPX}\cdot$. This results in forming a biradical product $\cdot\text{DPX-CH}_2\text{-CHX}\cdot$ whose further reactivity might be easily anticipated. Since the path A leads to a biradical product this mechanism should cause the copolymerization of such modified species ($\cdot\text{DPX-CH}_2\text{-CHX}\cdot$) and remaining para-xylylene dimers.

An alternative route for the path A leading to the $\cdot\text{DPX-CHX-CH}_2\cdot$ instead of $\cdot\text{DPX-CH}_2\text{-CHX}\cdot$ was also examined for a series of reactants. It was found that this route

(indicated as A' on Figure 2) leads to higher kinetic barriers (by 4-8 kcal/mol) and therefore we limited our further investigation to the previously considered route termed A in Figure 2.

The kinetic barriers found for the mechanism operating along the path A are relatively small. The smallest barriers for the mechanism A were found to be lower than 2 kcal/mol (for ethylene substituted with two CN groups, NO_2 , COOCHCl_2 , and COOC_6F_5 group, see Table 3). The activation barriers for the mechanism A never exceed 13 kcal/mol (for the species considered).

The general trend that can be observed is that the height of the kinetic barrier is related to the intuitive electronegativity of the X group (where X stands for the functional group in the $\text{CH}_2=\text{CHX}$ reactant). However, it should be stressed that there is no precise definition of the electronegativity of the chemical species built of more than one atom, and therefore it does not seem possible to formulate any convincing conclusions in this matter. The only hypothesis that might be originated is that an increase of the electronegativity of the X group causes a decrease of a corresponding kinetic barrier for the path A .

Despite the lack of the well-established electronegativity scale for molecular systems, one may try to connect the obtained kinetic barriers with the Hammett constants³⁶. Indeed, the Hammett constant for the NO_2 substituent is the largest (among the species considered) and reads 0.71 which is consistent with the fact that the kinetic barrier for $\text{CH}_2=\text{CHNO}_2$ reacting with the $\cdot\text{DPX}\cdot$ is very low (1.5 kcal/mol).

As far as the thermodynamic barriers for path A are concerned, we found the overall process to be exothermic in all cases considered (see Figure 3 where the representative energy profile is depicted).

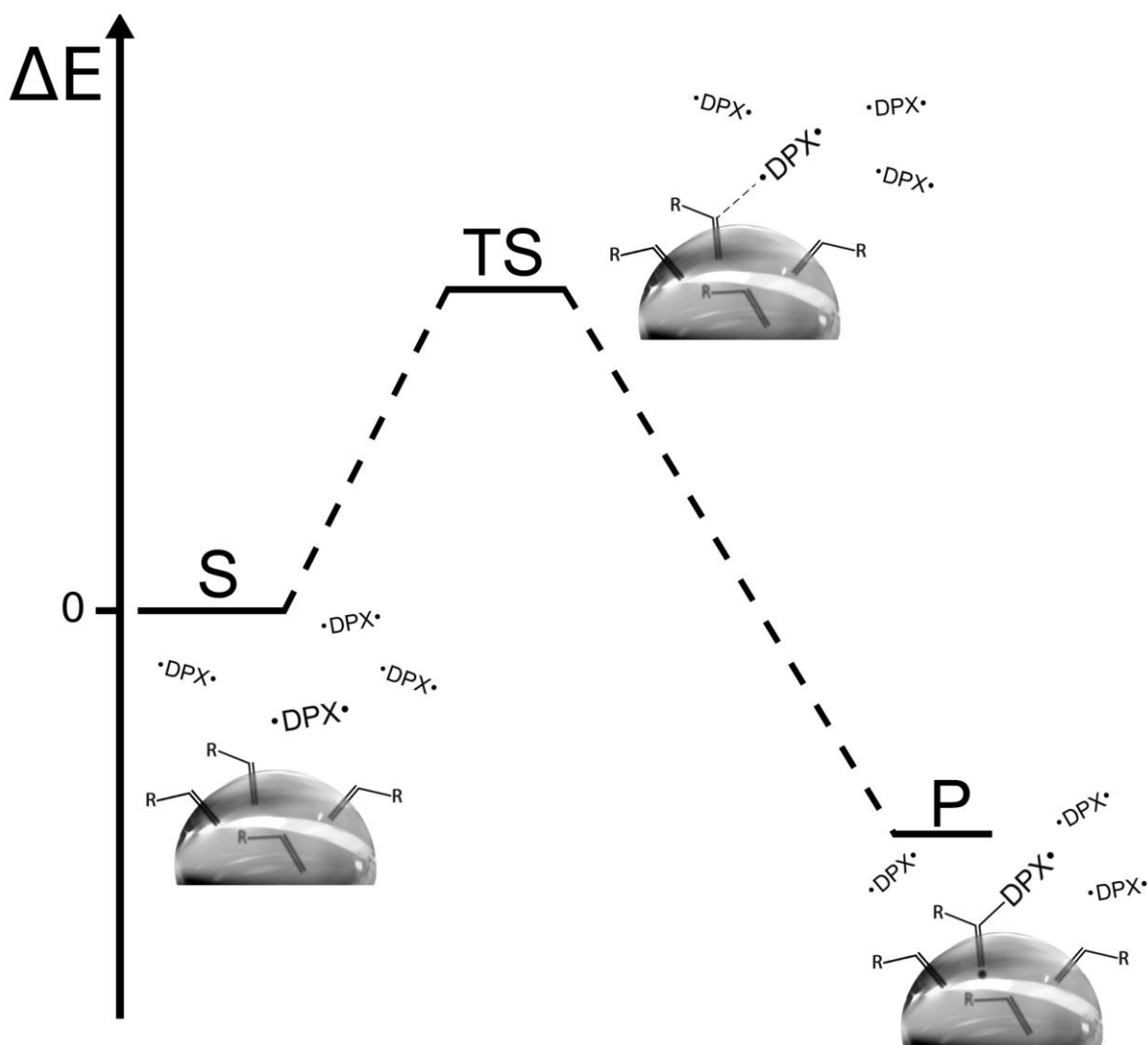


Figure 3. The schematic energy profile for the reaction of $\cdot\text{DPX}\cdot$ with a substrate containing substituted vinyl group (depicted here as sticking out of a liquid droplet) according to the path A (via the transition state).

For example, the resulting $\cdot\text{DPX-CH}_2\text{-CHX}\cdot$ biradical system is lower in energy than the reactants (i.e., $\cdot\text{DPX}\cdot$ and $\text{CH}_2=\text{CHX}$) by 13.0, 17.7, and 19.3 kcal/mol for $\text{X} = \text{Br}, \text{NO}_2, \text{C}_6\text{F}_5$ respectively (see Table 3).

The rate constants (\mathbf{k}) for the corresponding reactions were calculated according to Eq.(1) at the $T=298.15$ K and gathered in Table 4 (where the activation entropies and enthalpies are also collected). The values of \mathbf{k}_{298} obtained for the $\text{CH}_2=\text{C}(\text{CN})_2$ is the largest and reads $1.156 \times 10^4 \text{ M}^{-1}\text{s}^{-1}$ and those for ethylene substituted with COOC_6H_5 , NO_2 , and COOCHCl_2 are also greater than $10^2 \text{ M}^{-1}\text{s}^{-1}$ (see Table 4) which indicates very fast rates of the reactions of parylene with these substrates. The rate constants found for the substrates

substituted with CN and C₆F₅ are a few orders of magnitude smaller (ca. 1.4 M⁻¹s⁻¹) but remain relatively large. The slowest rates we predict for the parylene reacting with the substrates possessing silazane substituents (~10⁻⁴ M⁻¹s⁻¹) which is comparable to the reference compound (ethylene, **k**₂₉₈=6.557×10⁻⁴ M⁻¹s⁻¹, see Table 4).

3.2.2. Mechanism through the intermediate with hydrogen-atom detached

The second mechanism considered (termed *B*), depicted in Figure 4, involves the transfer of a hydrogen atom from the CH₂=CHX to the ·DPX·. This process requires surmounting of a certain kinetic barrier (whose height depends on the CH₂=CHX species since the other reactant remains unchanged). The resulting pair of radicals (doublet states) ·CH=CHX and ·DPXH may easily react with each other in the following step with no kinetic barrier. As a consequence, the closed-shell singlet state product is formed at the end of the path *B*. Therefore, the mechanism *B* quenches the reaction channel while the previously described route *A* (involving the π-bond cleavage, see the preceding subsection) leads to further polymerization or copolymerization of the resulting product due to its radical character.

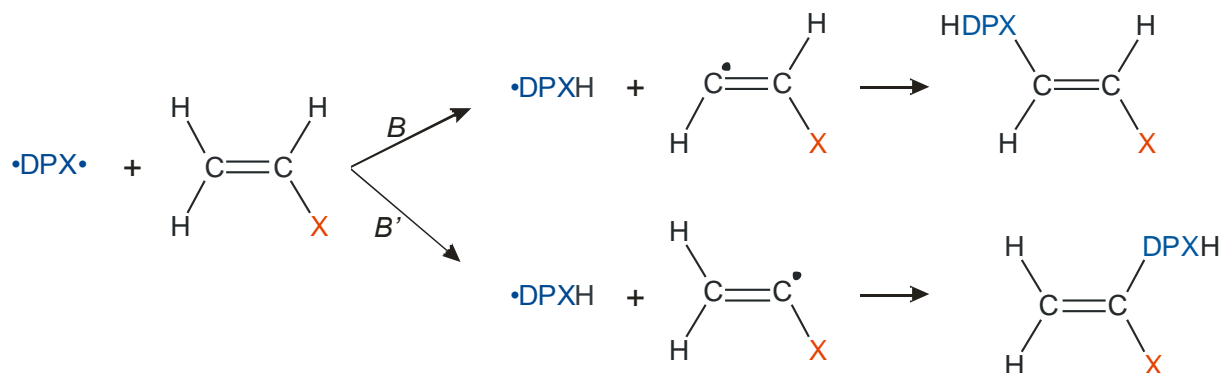


Figure 4. Mechanism *B* / *B'* involving the transfer of hydrogen atom

An alternative route for the path *B* leading to the CH₂=CX· instead of ·CH=CHX intermediate product (and consequently to a different final product) was also examined for a series of reactants. It was found that this route (indicated as *B'* in Figure 4) leads to very similar kinetic barriers to those obtained for the route *B* (within 1 kcal/mol) and therefore we limited our further investigation to the previously considered route termed *B* in Figure 4.

Both the DFT (B3LYP) and Hartree-Fock calculations indicate that the overall reaction which undergoes according to the path *B* is thermodynamically favorable (see Figure

5 where the representative energy profile is depicted). This conclusion has been formulated on the basis of the fact that the energy of the product is always significantly lower than that of the reactants (i.e., $\cdot\text{DPX}\cdot$ and $\text{CH}_2=\text{CHX}$). This reactants/products energy difference was found to be in the 63-67 kcal/mol range at the DFT level (22-26 kcal/mol while the HF method was employed).

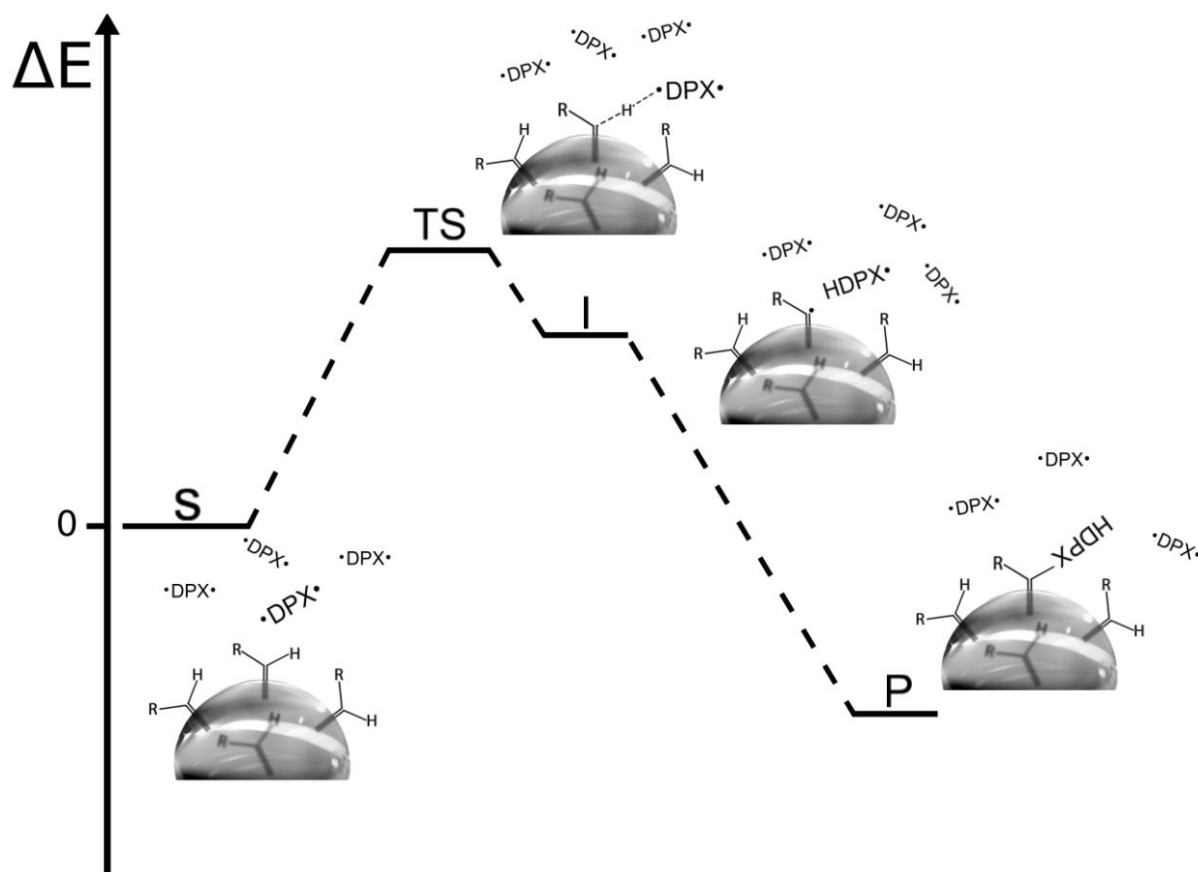


Figure 5. The schematic energy profile for the reaction of $\cdot\text{DPX}\cdot$ with a substrate containing substituted vinyl group (depicted here as sticking out of a liquid droplet) according to the path B (via the transition state and the intermediate products).

This indicates that the mechanism described by the route B should be thermodynamically favorable if the corresponding kinetic barriers are surmounted (see Table 3). However, the kinetic barriers that need to be overcome when the path B is operating are relatively high. The B3LYP results indicate that the smallest barriers (ca. 24 kcal/mol) occur for the ethylene substituted with the Cl or Br atoms or with $\text{Si}(\text{CH}_3)_2\text{-NH-SiHCH}_3\text{-NH-CH}_3$, and $\text{SiNH}_2\text{CH}_3\text{-NH-SiHCH}_3\text{-NH-CH}_3$ silazane groups. Typically, the activation barriers for the species considered are in the narrow 24-28 kcal/mol range (B3LYP), however, they seem



much higher (usually 30-40 kcal/mol) when the electron correlation effects are neglected (see the HF results given in parenthesis in Table 3).

Similarly to the general trend observed for the species reacting according to the path *A*, the height of the kinetic barrier seems to be related to the electronegativity of the X group in the CH₂=CHX reactant involved. An increase of the electronegativity of the X group causes a decrease of a corresponding kinetic barrier for the path *B* which is consistent with the chemical intuition that a detachment of the hydrogen atom from ethylene derivative should be easier if this molecule is substituted with the electronegative groups.

We also observed that the height of the kinetic barrier decreases when the reactant enters into conjugation with electrons of double bonds (styrene, perfluoro styrene, acrylate), as it was previously observed by Evans et al.²⁴.

The correlation between the kinetic barrier heights for the path *A* and the Hammett substituent constants (σ_m) is not straightforward. Namely, the Cl and Br substituents (σ_m equals to 0.37 and 0.39, respectively) lead to slightly lower barriers than the CN group ($\sigma_m=0.56$) while one could expect the opposite.

As far as the calculating rate constants are concerned, we found that all the reactions described by the path *B* are characterized by very small k_{298} values (in the 10⁻¹¹-10⁻¹⁴ M⁻¹s⁻¹ range, see Table 4) which is caused primarily by the large values of activation enthalpies (exceeding 22 kcal/mol in all cases studied). Hence, we conclude that the rate constants calculated for the processes that undergo according to the path *B* and requiring the H atom transfer are ca. 7-10 orders of magnitude smaller than those found when the path *A* is operating.

4. Conclusions

The LPCVD process of parylene with simultaneous reactions involving substrate molecules seems to be new functionalization fashion of thin layers in materials chemistry. In this means the critically important increase and improvement of the reaction capabilities of parylene is the main problem from materials chemistry point of view. Theoretical studies on the reactions of parylene with vinyl molecules revealed practical information for further exploration of surface-engineered templates in thin-films coatings. In particular, the MCSCF calculations show that:

- i. Both triplet and singlet state of biradical di-p-xylylene might exist during the polymerization process in gas phase and both seem to be capable of reacting with vinyl molecules.
- ii. The singlet state of a biradical p-xylylene dimer is multiconfigurational. The π and π^* orbitals of two aromatic rings of the dimer should be taken into account while performing calculations on the reaction energy profiles.

In addition, four mechanisms of reactions of biradical di-p-xylylene and molecules containing double bond between carbon atoms have been examined by means of quantum chemical methods. Appropriate stationary point structures were found and relative transition state energies were summarized in Table 3 while the corresponding rate constants were collected in Table 4. The results obtained led us to the following conclusions:

- i. The kinetic barriers that need to be overcome for the path *A* (π -bond cleavage) are small (<13 kcal/mol) with the highest value for the $\text{H}_2\text{C}=\text{CHCl}$ (12.4 kcal/mol) and the lowest for the $\text{H}_2\text{C}=\text{C}(\text{CN})_2$ compound (0-1 kcal/mol). The corresponding rate constants for these processes were calculated to be in the $\sim 10^4$ - $10^{-4} \text{ M}^{-1}\text{s}^{-1}$ range. Such reaction leads to copolymers as the product remains biradical.
- ii. The kinetic barriers for the mechanism *B* (hydrogen atom transfer) are relatively high (24-28 kcal/mol) which decreases the probability of this process despite of the large thermodynamic barriers (63-67 kcal/mol). The corresponding rate constants for these processes were calculated to be in the $\sim 10^{-11}$ - $10^{-14} \text{ M}^{-1}\text{s}^{-1}$ range. This channel quenches the polymerization process since it leads to closed-shell (i.e., non-radical) products.
- iii. The height of the kinetic barrier decreases when the reactant possesses either a strongly electronegative group or a larger number of double bonds which allows for delocalization of the π -electrons.
- iv. The barriers found for the reactions of $\cdot\text{DPX}\cdot$ with molecules containing double bonds between carbon atoms depend on the operating mechanism and in the most promising case (route *A*) are equal or similar to the barriers of propagation of polymer chains (the kinetic barriers found by Smalara et al.³⁴ for propagation of parylene chains are low and equal about 3 kcal/mol).
- v. All the kinetic barriers found might be reduced by choosing certain electronegative substituents. By the appropriate choice the kinetic barrier can be reduced to almost 0 kcal/mol which makes the reaction possible during polymerization of parylenes at room temperature.



5. Acknowledgements

This work was supported by STREP n°033201 funded by the European Commission within the 6th Framework Program as well as by the Polish Ministry of Science and Education, grant number 399/6PRUE/2007/7. The computer time provided by the Academic Computer Center in Gdansk (TASK) is also gratefully acknowledged.

Table 1. Energy differences (kcal/mol) between triplet and singlet state of biradical DPX in various MCSCF calculations.

MCSCF	E(triplet) – E(singlet)
C₂-symmetry imposed	
MCSCF(14,14) (single and double excitations)	-97.95
CASSCF(2,2)	-129.00
No symmetry constraints (C₁-symmetry)	
MCSCF(14,14) (single and double excitations)	-1.35
CASSCF(2,2)	0.01

Table 2. Dominant configuration state functions (CSFs) of singlet and triplet state of biradical DPX after full geometry optimization. Only CSFs with coefficients larger than 0.1 in absolute value are presented.

C₂-symmetry imposed		
MCSCF(14,14) with single and double excitations		
State multiplicity	Coefficients	CSF
triplet	0.9023	22222211000000
singlet	0.4773	22221221000000
	-0.4593	22222112000000
	-0.1313	22212212000000
	0.2640	22221211001000
	-0.1628	22222201001000
	-0.2632	22221211100000
	0.1789	22222201100000
	-0.3639	22222111000100
	0.2388	22222210000100
CASSCF(2,2)		
State multiplicity	Coefficients	CSF
triplet	1.000	11
singlet	1.000	11
No symmetry constraints (C₁-symmetry)		
MCSCF(14,14) with single and double excitations		
State multiplicity	Coefficients	CSF
triplet	0.9055	22222211000000
singlet	-0.6274	22222202000000
	0.6444	22222220000000
	-0.1514	22221211010000
	-0.1545	22222111100000
CASSCF(2,2)		
State multiplicity	Coefficients	CSF
triplet	1.0000	11
singlet	-0.7030	02
	0.7112	20

Table 3. Kinetic and thermodynamic barriers for the reactions of para-xylylene dimer with the CH₂=CHX molecule (see first column for the definition of the substituent X). The Hartree-Fock calculated values are given in parentheses. All energies in kcal/mol.

-X	path A		path B	
	Kinetic barrier DFT (HF)	Thermodynamic barrier DFT (HF)	Kinetic barrier DFT (HF)	Thermodynamic barrier DFT (HF)
—H	10.2 (17.5)	-9.1 (1.0)	27.3 (41.9)	-63.8 (-23.6)
—silazaneB ^a	8.6 (16.2)	-11.6 (-0.8)	24.5 (41.2)	-63.3 (-22.0)
—silazaneA ^b	9.6 (17.5)	-10.9 (-0.1)	24.7 (41.1)	-63.1 (-22.2)
—Br	7.9 (15.1)	-13.0 (-2.7)	24.2 (40.2)	-66.3 (-24.0)
—Cl	12.4 (18.7)	-15.6 (-5.3)	25.1 (40.7)	-63.9 (-24.3)
—COOC ₆ F ₅	2.0 (11.4)	-18.2 (-12.7)	27.2 (17.6)	-65.7 (-25.5)
=C(CN) ₂	0.0 (3.9)	-25.5 (-21.0)	27.3 (36.7)	-66.7 (-25.5)
—NO ₂	1.5 (0.0)	17.7 (-4.1)	27.4 (42.6)	-65.5 (-24.5)
—COOCHCl ₂	2.0 (11.8)	-18.0 (-6.4)	27.4 (41.2)	-65.7 (-25.6)
—COOC ₄ H ₈ OH	3.9 (12.7)	-17.3 (-5.3)	27.5 (41.4)	-64.8 (-24.9)
—C ₆ F ₅	4.6 (3.2)	-19.3 (-17.7)	27.7 (33.1)	-64.4 (-24.3)
—CF ₃	6.4 (15.2)	-12.4 (-1.2)	27.8 (42.9)	-64.9 (-23.7)
—C ₆ H ₅	6.5 (5.0)	-18.2 (-16.1)	27.9 (43.2)	-63.6 (-23.5)
—CN	4.8 (10.1)	-18.4 (-12.8)	27.9 (39.9)	-65.0 (-23.7)

^a silazaneB = SiNH₂CH₃-NH-SiHCH₃-NH-CH₃

^b silazaneA = Si(CH₃)₂-NH-SiHCH₃-NH-CH₃

Table 4. The B3LYP/6-31G enthalpies (ΔH^\ddagger) and entropies (ΔS^\ddagger) of activation and the resulting rate constants k_{298} (calculated for $T=298.15$ K) for the reactions of para-xylylene dimer with the $\text{CH}_2=\text{CHX}$ molecule (see first column for the definition of the substituent X). Rate constants in s^{-1} , enthalpies in $\text{kcal}\cdot\text{mol}^{-1}$, entropies in $\text{cal}\cdot\text{mol}^{-1}\cdot\text{K}^{-1}$.

-X	Path A			Path B		
	ΔH^\ddagger	ΔS^\ddagger	$k_{298} [\text{s}^{-1}]$	ΔH^\ddagger	ΔS^\ddagger	$k_{298} [\text{s}^{-1}]$
—H	11.634	-34.084	$6.557 \cdot 10^{-4}$	25.542	-26.170	$2.247 \cdot 10^{-12}$
—silazaneB ^a	10.157	-39.320	$5.689 \cdot 10^{-4}$	23.016	-30.495	$1.811 \cdot 10^{-11}$
—silazaneA ^b	11.149	-37.897	$2.182 \cdot 10^{-4}$	23.218	-32.869	$3.901 \cdot 10^{-12}$
—Br	9.484	-36.467	$7.445 \cdot 10^{-3}$	22.861	-29.684	$3.539 \cdot 10^{-11}$
—Cl	10.034	-35.006	$6.137 \cdot 10^{-3}$	23.759	-29.196	$9.938 \cdot 10^{-12}$
—COOC ₆ F ₅	4.242	-31.431	$6.528 \cdot 10^2$	26.416	-25.801	$6.190 \cdot 10^{-13}$
—(CN) ₂	1.452	-35.078	$1.156 \cdot 10^4$	26.990	-28.723	$5.400 \cdot 10^{-14}$
—NO ₂	3.236	-37.645	$1.564 \cdot 10^2$	26.402	-29.373	$1.050 \cdot 10^{-13}$
—COOCHCl ₂	3.649	-35.831	$1.940 \cdot 10^2$	25.998	-29.212	$2.254 \cdot 10^{-13}$
—COOC ₄ H ₈ OH	5.561	-39.971	$9.586 \cdot 10^{-1}$	26.027	-31.803	$5.823 \cdot 10^{-14}$
—C ₆ F ₅	6.118	-37.290	1.443	26.153	-30.663	$8.354 \cdot 10^{-14}$
—CF ₃	26.412	-31.835	$9.463 \cdot 10^{-2}$	26.513	-30.656	$4.566 \cdot 10^{-14}$
—C ₆ H ₅	7.963	-36.516	$9.463 \cdot 10^{-2}$	26.412	-31.835	$2.992 \cdot 10^{-14}$
—CN	6.360	-36.432	1.477	26.687	-28.662	$9.285 \cdot 10^{-14}$

^a silazaneB = $\text{SiNH}_2\text{CH}_3\text{-NH-SiHCH}_3\text{-NH-CH}_3$

^b silazaneA = $\text{Si(CH}_3)_2\text{-NH-SiHCH}_3\text{-NH-CH}_3$

Captions for figures

Figure 1. Singly-occupied biradical orbitals (symmetrical (**a**) and antisymmetrical (**b**)) of di-*p*-xylylene obtained at the MCSCF(14,14) level with single and double excitations with the natural orbitals basis. The occupation numbers are as follows: singlet-state dimer optimized without symmetry constraints - orbital **a**: 1.03; orbital **b**: 0.97, optimized with the C_2 -symmetry imposed – orbital **a**: 1.24; orbital **b** 1.23; in the case of triplet-state dimer both orbitals are singly-occupied.

Figure 2. Mechanism A / A' involving the π -bond cleavage

Figure 3. The schematic energy profile for the reaction of $\cdot\text{DPX}\cdot$ with a substrate containing substituted vinyl group (depicted here as sticking out of a liquid droplet) according to the path A (via the transition state).

Figure 4. The mechanism B / B' involving the transfer of hydrogen atom

Figure 5. The schematic energy profile for the reaction of $\cdot\text{DPX}\cdot$ with a substrate containing substituted vinyl group (depicted here as sticking out of a liquid droplet) according to the path B (via the transition state and the intermediate products).

References

- ¹ M. Szwarc, *Discuss. Faraday Soc.* 2 (1947) 46.
- ² W. F. Gorham, *J. Polym. Sci. Part A-1: Polym. Chem.* 4 (1966) 3027.
- ³ J. B. Fortin, T. M. Lu, *Chemical vapor deposition polymerization: the growth and properties of parylene thin films*; Kluwer: Boston, 2004.
- ⁴ L. A. Errede, M. Szwarc, *Quart. Rev. (London)* 12 (1958) 301.
- ⁵ H. Keppner, M. Benkhaira, WO/2006/063955.0.
- ⁶ W. F. Gorham, US Pat. 3342754, 1967 (to Union Carbide Corp.).
- ⁷ J. Lahann, M. Balcells, H. Lu, T. Radon, K. F. Jensen, R. Langer, *Anal. Chem.* 75 (2003) 2117.
- ⁸ S. Takayama, E. Ostuni, P. LeDuc, K. Naruse, D. E. Ingber, G. M. Whitesides, *Nature* 411 (2001) 1016.
- ⁹ H. Y. Chen, Y. Elkasabi, J. Lahann, *J. Am. Chem. Soc.* 128 (2006) 374.
- ¹⁰ Beach, W.F., "Xylylene polymers" in *Encyclopedia of Polymer Science and Technology*, edited by H. F. Mark, John Wiley and Sons Inc., New York (2004), pp. 587-626.
- ¹¹ H. Hopf, *Angew. Chem. Int. Ed.* 47 (2008) 9808.
- ¹² J. Lahann, *Polym. Int.* 55 (2006) 1361.
- ¹³ M. Cetinkaya, N. Malvadkar, M. C. Demirel, *J. Polym. Sci.: Part B: Polym. Phys.* 46 (2008) 640.
- ¹⁴ L. A. Errede, M. Szwarc, *Q. Rev. Chem. Soc.* 12 (1958) 301.
- ¹⁵ M. Szwarc, *Polym. Eng. Sci.* 16 (1976) 473.
- ¹⁶ A. Bolognesi, Ch. Botta, A. Andicsova, U. Giovanella, S. Arnautov, J. Charmet, E. Laux, H. Keppner, *Macromol. Chem. Phys.* (2009), 210, DOI: 10.1002/macp.200900321
- ¹⁷ *Polymer Handbook*, 3rd ed., J. Brandrup, E. H. Immergut, Eds. John Wiley, New York, (1989).
- ¹⁸ J. Filley, J. T. McKinnon, D. T. Wu, *Macromol.* 35 (2002) 3731.
- ¹⁹ K. F. O'Driscoll, T. Yonezawa, *Rev. Macromol. Chem.* 1 (1966) 1.
- ²⁰ K. F. O'Driscoll, T. Yonezawa, T. Higashimura, *J. Macromol. Sci. Chem.* 1 (1966) 1.
- ²¹ T. Minato, S. Yamabe, H. Fujimoto, K. Fukui, *Bull. Chem. Soc. Jpn.* 51 (1978) 1.
- ²² T. Yonezawa, K. Hayashi, C. Nagata, S. Okamura, K. Fukui, *J. Polym. Sci.* 14 (1954) 312.
- ²³ A. Tachibana, K. Nakamura, *J. Am. Chem. Soc.* 117 (1995) 3605.
- ²⁴ M. G. Evans, J. Gergely, E. C. Seaman, *J. Polym. Sci.* 3 (1948) 866.
- ²⁵ F. W. Sears, M. W. Zemansky, *University Physics*, Addison-Wesley Publishing Company, Sixth ed., 1982.
- ²⁶ A. D. McLean, G. S. Chandler, *J. Chem. Phys.* 72 (1980) 5639.
- ²⁷ R. Krishnan, J. S. Binkley, R. Seeger, J. A. Pople, *J. Chem. Phys.* 72 (1980) 650.
- ²⁸ C. Lee, W. Yang, R. G. Parr, *Phys. Rev. B* 37 (1988) 785.
- ²⁹ A. D. Becke, *Phys. Rev. A* 38 (1988) 3098.
- ³⁰ T. H. Lowry, K. S. Richardson, *Mechanism and Theory in Organic Chemistry*, 2nd ed.; Harper & Row: New York, 1981; p 194.
- ³¹ Gaussian 03, Revision A.1, M. J. Frisch, G. W. Trucks, H. B. Schlegel, G. E. Scuseria, M. A. Robb, J. R. Cheeseman, J. A. Montgomery, Jr., T. Vreven, K. N. Kudin, J. C. Burant, J. M. Millam, S. S. Iyengar, J. Tomasi, V. Barone, B. Mennucci, M. Cossi, G. Scalmani, N. Rega, G. A. Petersson, H. Nakatsuji, M. Hada, M. Ehara, K. Toyota, R. Fukuda, J. Hasegawa, M. Ishida, T. Nakajima, Y. Honda, O. Kitao, H. Nakai, M. Klene, X. Li, J. E. Knox, H. P. Hratchian, J. B. Cross, C. Adamo, J. Jaramillo, R. Gomperts, R. E. Stratmann, O. Yazyev, A. J. Austin, R. Cammi, C. Pomelli, J. W. Ochterski, P. Y. Ayala, K. Morokuma, G. A. Voth, P. Salvador, J. J. Dannenberg, V. G. Zakrzewski, S. Dapprich, A. D. Daniels, M. C. Strain, O. Farkas, D. K. Malick, A. D. Rabuck, K. Raghavachari, J. B. Foresman, J. V. Ortiz, Q. Cui, A.

G. Baboul, S. Clifford, J. Cioslowski, B. B. Stefanov, G. Liu, A. Liashenko, P. Piskorz, I. Komaromi, R. L. Martin, D. J. Fox, T. Keith, M. A. Al-Laham, C. Y. Peng, A. Nanayakkara, M. Challacombe, P. M. W. Gill, B. Johnson, W. Chen, M. W. Wong, C. Gonzalez, and J. A. Pople, Gaussian, Inc., Pittsburgh PA, 2003.

³² GAMESS, General Atomic and Molecular Electronic Structure System, M. W. Schmidt, K. K. Baldridge, J. A. Boatz, S. T. Elbert, M. S. Gordon, J. H. Jensen, S. Koseki, N. Matsunaga, K. A. Nguyen, S. J. Su, T. L. Windus, M. Dupuis, J. A. Montgomery, *J. Comput. Chem.* 14 (1993) 1347.

³³ M. Bobrowski, A. Liwo, S. Oldziej, D. Jeziorek, T. Ossowski, *J. Am. Chem. Soc.* 122 (2000) 8112.

³⁴ K. Smalara, A. Gieldon, M. Bobrowski, J. Rybicki, C. Czaplewski, sent for publication in *J. Phys. Chem.*

³⁵ M. Szwarc, *Polym. Eng. Sci.* 16 (1976) 473.

³⁶ C. Hansch, A. Leo, R. W. Taft, *Chem. Rev.* 91 (1991) 165.

Figure 1
[Click here to download high resolution image](#)

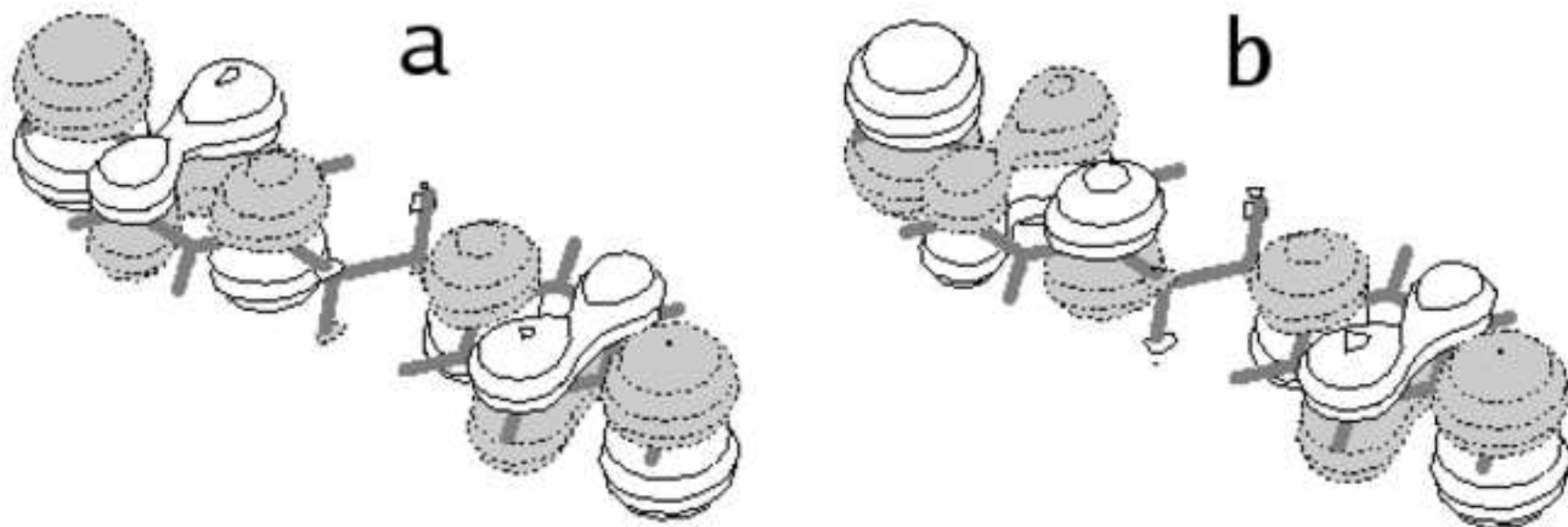


Figure 2
[Click here to download high resolution image](#)

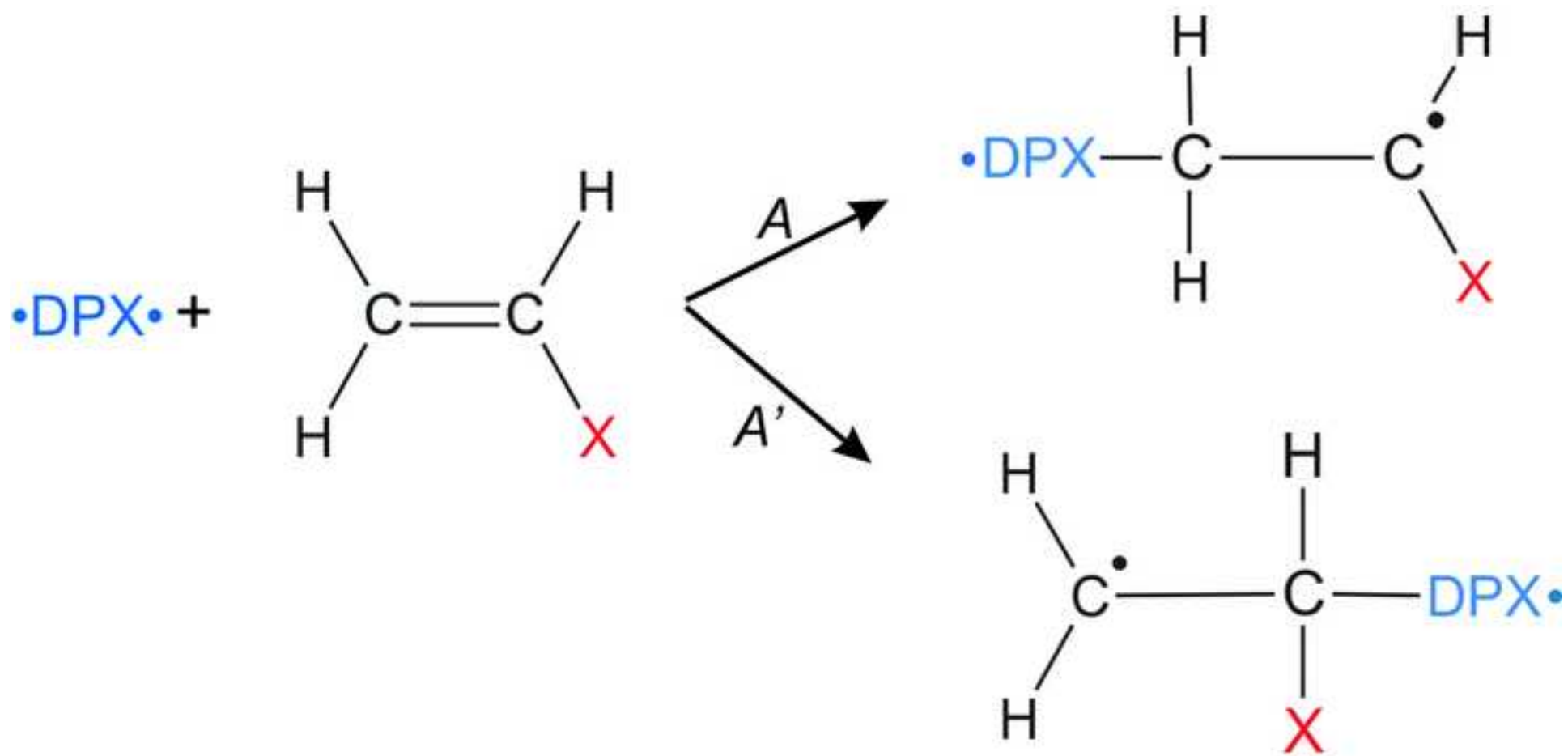


Figure 3
[Click here to download high resolution image](#)

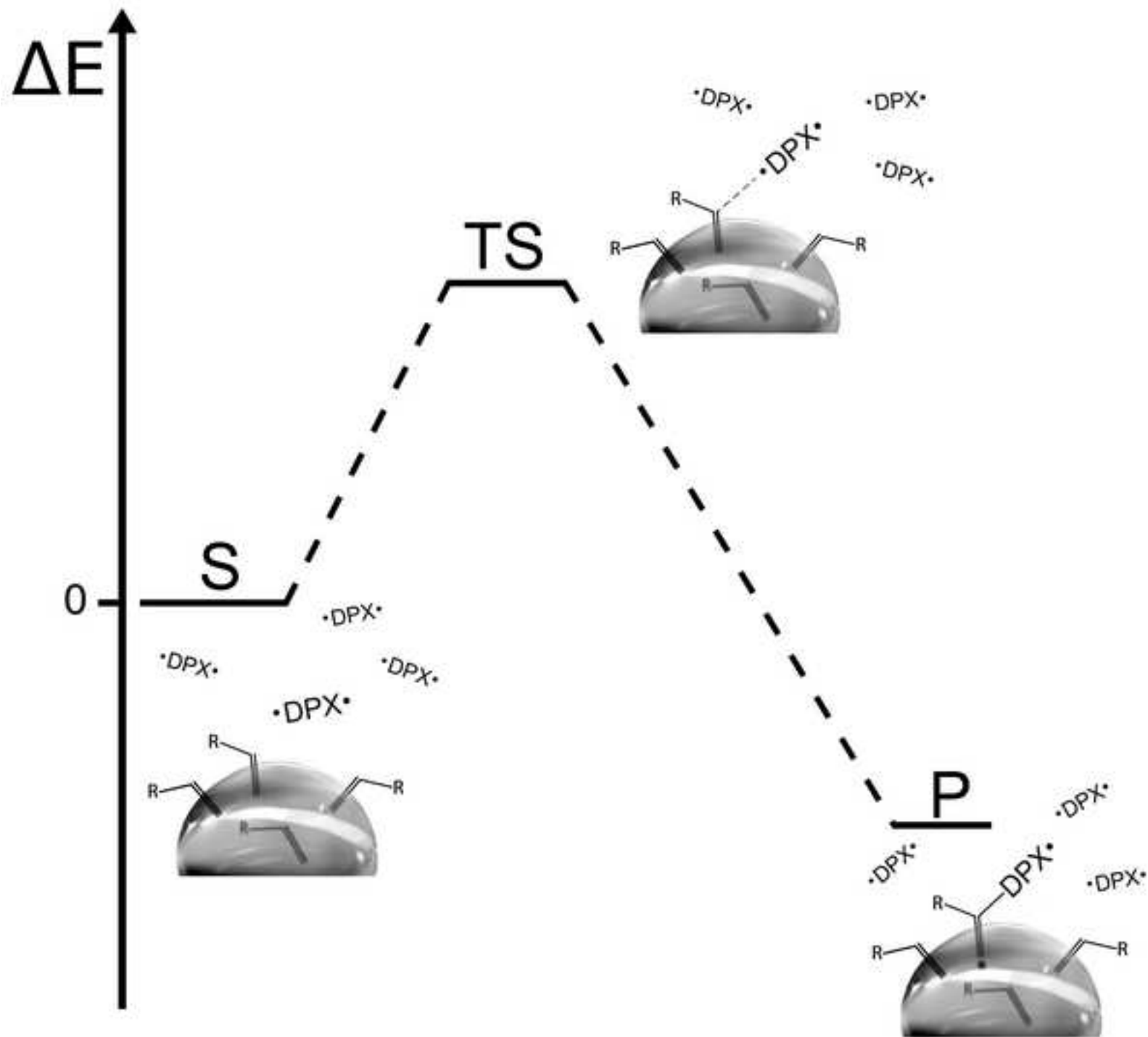


Figure 4
[Click here to download high resolution image](#)

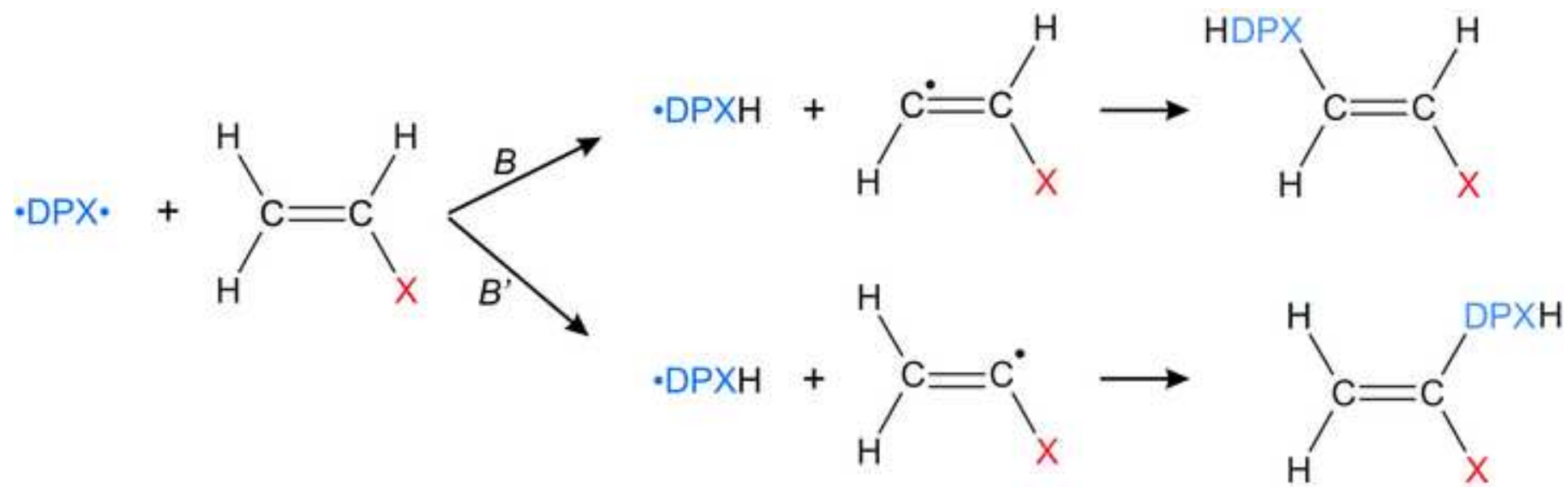


Figure 5
[Click here to download high resolution image](#)

